



Hydrodynamic characteristics and flow regime investigation of an anaerobic baffled reactor (ABR)

Mehdi Hassanvand Jamadi^a, Abolghasem Alighardashi^{b,*}

^aOmrab Canada Inc. 290 Buena Vista Road, Ottawa, Ontario, K1M 0V7, Canada, email: hasanvand@omrab.net

^bFaculty of Civil, Water & Environmental Engineering, Shahid Beheshti University, P.O. Box: 16765-1719, Zip Code: 1658953571, Tehran, Iran, Tel. +982173932467, Fax +982177006660, email: a_ghardashi@sbu.ac.ir

Received 24 June 2017; Accepted 4 December 2017

ABSTRACT

This research investigates the hydrodynamic characteristics of a 6-liter and 8-compartment anaerobic baffled reactor (ABR) including dead volumes, short-circuiting, and reactor's flow regime. Maximum dead volume was approximately 11% of total volume while the short-circuiting was not considerable. The minimum number of reactor's equivalent tanks in series (TIS) was estimated to be 10. The lowest hydraulic efficiency was 80%. The reactor's performance was similar to that of the ideal plug flow reactors, due to its large number of compartments. In addition, the minimum plug flow volume was about 78% of total reactor volume. For better assessment of the flow regime, the "plug flow index" (PI) was proposed and the reactors were classified based on this index. Since PI was more than 0.75, the reactor was classified in the category of "Plug Flow Reactors". Variations in a number of environmental parameters such as temperature, dissolved solids, and suspended solids were considered. The results showed that a decrease in temperature and addition of high amounts of dissolved solids make the reactor an ideal plug flow reactor while suspended solids do not change the flow regime.

Keywords: Anaerobic baffled reactor; Dead volume; Hydrodynamics; Plug flow index

1. Introduction

The anaerobic baffled reactor (ABR) is defined as an upflow anaerobic sludge blanket (UASB) compartmentalized with baffles. Sludge is suspended in the upward section, and this reactor is capable of treating wastewaters with high organic loads. The reactor produces very low excess sludge and does not require a final sedimentation tank [1].

The function of ABR is based on reactor hydrodynamics and its physical structure is designed such that flow direction and velocity sequentially change inside the reactor. The high flow velocity in the downward section eliminates the possible sediments or the hydraulic channelization phenomenon and prevents the decrease in reactor's effective volume. The end of each compartment splitting blade has a 45° flexure to conduct the flow into the reactor's central parts, which allows for a better contact between the passing wastewater and the existing microorganisms [2].

In addition, due to the necking under the curved blade, flow velocity increases considerably in this section. Consequently, if the materials inside the upward section settle, the high velocity in this section prevents any possible obstruction.

Some studies have been conducted on anaerobic baffled reactors from the hydrodynamic point of view. A research studied the hydraulic unsteady flow and its effect on hydrodynamic characteristics of an ABR with three compartments and a primary sedimentation tank [3]. In another study [4], the hydrodynamic characteristics of two ABRs, namely the plane folded plate reactor and the opposite folded plate reactor, were studied and compared. Flow hydrodynamics was examined in a modified ABR with four compartments with different dimensions [5]. Also, the performance of an ABR used for landfill waste leachate treatment was evaluated with different values of hydraulic retention time (HRT) [6]. In a recent essay, various reactors of equal effective volume were adopted to investigate the flow patterns of the ABR. Its results showed that an increase in ABR compart-

*Corresponding author.

ments resulted in the decrease in back-mixing, which made the fluid in the reactor reach a plug flow state [7]. Despite the significance of studies on the hydrodynamics of ABRs, they pale compared to the works conducted on biological processes [8,9]. Moreover, in most of these studies, reactors with fewer compartments were studied. Hence, further investigations are necessary on the hydrodynamics of these reactors, especially with more compartments.

A reactor with a large number of compartments was used in this research and its hydrodynamic characteristics were studied. The dead space, plug flow, and completely mixed volumes inside the reactor, short-circuiting, and hydraulic efficiency are indices considered in this research. The reactor's flow regime, which plays an important role in the operation of the reactor, is discussed in this work. To assess flow regime, the tanks in series (TIS) and axial dispersion (AD) models were used, followed by examining the conformity of the models' results to experimental results. The AD model is sensitive to boundary conditions when the dispersion is high and using improper boundary conditions results in deceptive conclusions. Since this point has not been considered precisely in previous similar studies, the focus of this work is on the importance of applying proper boundary conditions and also the consequences of using incorrect boundary conditions. Due to the lack of a comprehensive and comparative criterion to exact compare of flow types inside reactors, "plug flow index" was introduced for better classification of reactors' flow regime. The effects of actual flow conditions and their variations on hydrodynamic parameters with changes in fluid temperature, solutes, and suspended solids content were also investigated.

2. Materials and methods

2.1. Reactor specifications

A laboratory scale reactor with 8 compartments and a total volume of 6 L was used in this research. Each com-

partment of the reactor was divided into the upward and downward sections (Fig. 1a). The length (and volume) of the upward section was 3 times the length (and volume) of the downward section [10].

2.2. RTD study

In this research, Rhodamine B was used as a tracer and then the retention time distribution (RTD) curve (Fig. 1b) was prepared. The mean retention time and variance were calculated for each curve using Eq. (1) and Eq. (2), respectively. Moreover, the normalized curve parameters were also calculated using Eqs. (3)–(6) [11]:

$$\bar{t}_c = \frac{\int_0^{\infty} tC(t)dt}{\int_0^{\infty} C(t)dt} \quad (1)$$

$$\sigma_t^2 = \frac{\int_0^{\infty} (t - \bar{t}_c)^2 C(t)dt}{\int_0^{\infty} C(t)dt} = \frac{\int_0^{\infty} t^2 C(t)dt}{\int_0^{\infty} C(t)dt} - \bar{t}_c^2 \quad (2)$$

$$\theta = \frac{t}{HRT} \quad (3)$$

$$C(\theta) = \frac{C(t)}{C_0} \quad (4)$$

$$\bar{\theta} = \frac{\bar{t}_c}{HRT} \quad (5)$$

$$\sigma_{\theta}^2 = \frac{\sigma_t^2}{t_c^2} \quad (6)$$

In the above equations, t is time, HRT is the theoretical hydraulic retention time, θ is normalized time, $C(t)$ is the concentration at time t , C_0 is nominalized concentration (which equals the mass of injected Rhodamine divided by

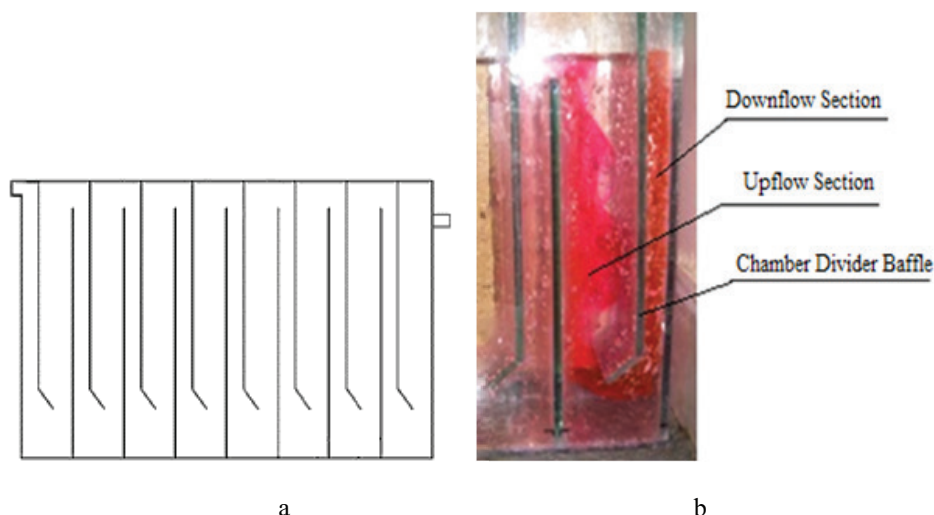


Fig. 1.(a) Schematic of studied reactor and (b) Tracer injection into the reactor.

reactor volume), and $C(\theta)$ is the normalized concentration at the normalized time θ . In addition, $\bar{\theta}$ denotes the reactor's normalized retention time and σ_θ^2 is the normalized variance.

2.3. Determining hydrodynamic indices

The reactor's effective and dead volumes are calculated by Eq. (7) and Eq. (8), respectively [3]. The short-circuiting is defined by Eq. (9) [11], where SCI represents the short-circuiting index and t_i is the time at which the first output tracer is observed.

$$e = \frac{\bar{t}_c}{HRT} \quad (7)$$

$$\frac{V_d}{V} = 1 - e \quad (8)$$

$$SCI = \frac{t_i}{HRT} \quad (9)$$

To detect the non-ideal flow regime in reactors, two tanks in series (TIS) and axial dispersion (AD) models are used. TIS and AD models are shown in Eq. (10) and Eq. (12), respectively [12,13].

$$C_\theta = \frac{N}{(N-1)!} (N\theta)^{N-1} e^{-N\theta} \quad (10)$$

$$N = \frac{1}{\sigma_\theta^2} \quad (11)$$

$$\frac{\partial C}{\partial \theta} = \left(\frac{D}{uL} \right) \frac{\partial^2 C}{\partial Z^2} - \frac{\partial C}{\partial Z} \quad (12)$$

$$\sigma_\theta^2 = \frac{2}{Pe} - \frac{2}{Pe^2} (1 - e^{-Pe}) \quad (13)$$

In the above equations, θ is normalized time, C_θ is the normalized concentration at the time θ , N indicates the number of TIS, D is axial dispersion coefficient, u is flow velocity, L is the characteristic length, and Z is the normalized length, which equals the length traveled by the flow at the time θ divided by reactor's length. Moreover, D/uL ($= d$) is dispersion number and is estimated by Eq. (13), where Pe is Péclet number and equals to the inverse of dispersion number ($Pe = 1/d = uL/D$).

For dispersion numbers bigger than 0.01, the solution to the differential Eq. (12) depends on the reactor's boundary conditions. If plug flow exists outside a boundary ($D = 0$) and flow disperses immediately within the boundary, the boundary is called a closed boundary. If the flow disperses equally inside and outside the boundary, the boundary is considered open. By solving the differential Eq. (12) for open boundaries, the following equation is obtained [12].

$$C_\theta = \frac{1}{2\sqrt{\pi\theta(D/uL)}} \exp\left[-\frac{(1-\theta)^2}{4\theta(D/uL)}\right] \quad (14)$$

The solution to the dispersion equation is more complicated for closed boundaries. For that type of reactors,

applying the boundary conditions of Eq. (15), the solution is converted to Eq. (16) [14].

$$C_1 = C_{x \rightarrow 0^+}, \quad \left(\frac{\partial C}{\partial x} \right)_{x \rightarrow L} = 0 \quad (15)$$

where C is concentration, C_1 is the concentration in upstream the input boundary, x is the distance from the inlet of the reactor, L is the reactor length, and t is time.

$$C_\theta = \sum_{n=1}^{\infty} \left[\frac{-\alpha_n^2}{\left(\frac{Pe}{2} + \left(\frac{Pe}{2} \right)^2 + \alpha_n^2 \right) \cos \alpha_n} \exp \left[\frac{Pe}{2} - \left[\frac{\left(\frac{Pe}{2} \right)^2 + \alpha_n^2}{Pe} \right] \theta \right] \right] \quad (16)$$

where α_n is the n -th root of the following transcendence equation:

$$\tan \alpha = \frac{-2\alpha}{Pe} \quad (17)$$

Those portions of the reactor in which the plug flow and completely mixed occur are calculated using Eq. (18) and Eq. (19), respectively [15]. Hydraulic efficiency as another reactor's hydraulic characteristic was investigated using Eq. (20) [16]:

$$\frac{V_p}{V} = \frac{\theta_{peak}}{\bar{\theta}} \quad (18)$$

$$\frac{V_m}{V} = 1 - \frac{V_p}{V} - \frac{V_d}{V} \quad (19)$$

$$\lambda = e \left(1 - \frac{1}{N} \right) \quad (20)$$

In the above equations, θ_{peak} shows the peak time of the RTD curve, $\bar{\theta}$ is the mean retention time, V_p is the plug flow volume, V_m is the completely mixed volume, V_d is the reactor's dead volume, V is the total reactor volume, λ is hydraulic efficiency, e is reactor's effective volume, and N is the number of tanks in series.

3. Results and discussion

3.1. Determining hydrodynamic indices

RTD curves are shown as solid lines in Fig. 2 for different times. Moreover, Table 1 presents the theoretical and experimental retention times for the resulting RTD curves. The differences between the theoretical and experimental retention times are caused by numerous factors such as the development of dead spaces.

Based on the calculated reactor's dead and effective volume values (Table 1), it could be stated that a considerable percentage of the ABR's volume is effective, and only a small portion is considered as hydraulic dead space (11% maximum). Grobicki and Stuckey [17] and Renuka et al. [18] also reported a very small hydraulic dead space for ABR (less than 8% and 15%, respectively). The largest dead space belongs to the retention time of 110 min, which accounts for 11% of the reactor's volume. A small

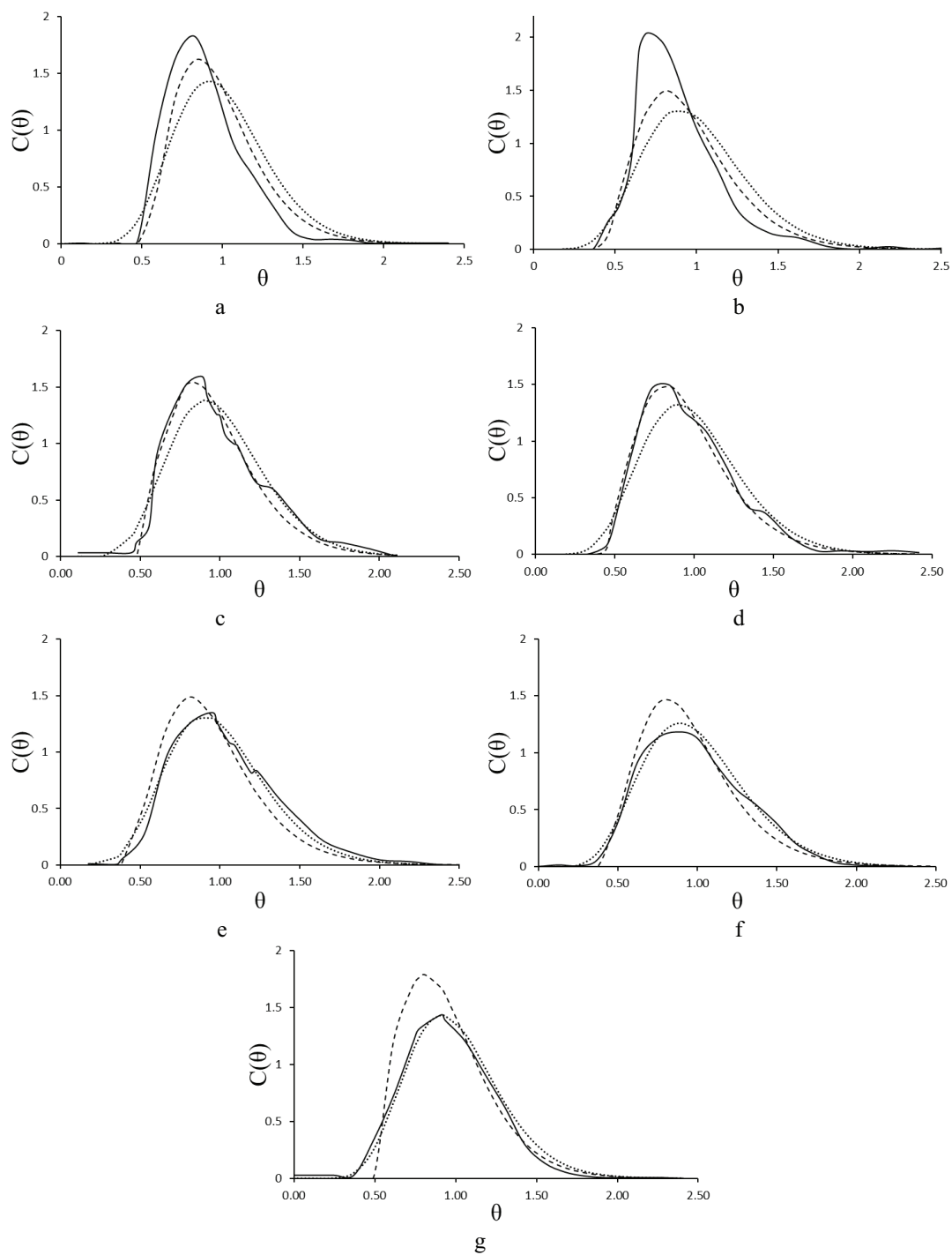


Fig. 2. Experimental RTD curves, AD model and TIS model for various HRTs (a: 93 min, b: 110 min, c: 180 min, d: 248 min, e: 284 min, f: 332 min, g: 366 min). The solid lines refer to experimental RTD curves, the dashed lines refer to AD model, and the dot lines refer to TIS model. $C(\theta)$: normalized concentration; θ : normalized time.

dead space is observed at other retention times that can be attributed to the uniform flow distribution inside the reactor. In general, it could be concluded that with a decrease in retention time and an increase in flow velocity (and Reynolds number), the hydraulic dead space increases. Other researchers have also obtained similar results [4,18,19,20].

However, there seems to be no exact relationship between retention time and dead space. Grobicki and Stuckey [17] also reported a similar finding. Since the dead space is small and the theoretical and experimental retention times are similar, the ABR's actual and design retention times are almost conforming.

Table 1
Resulted indices for various HRTs

HRT (min)	\bar{t}_c (min)	σ_θ^2	e (%)	V_d (%)	SCI
93	83.45	0.07757	89.93	10.07	0.527
110	97.74	0.09869	88.86	11.14	0.409
180	177.90	0.08877	98.83	1.17	0.45
248	239.94	0.09797	96.75	3.25	0.333
284	292.02	0.09917	102.82	–	0.342
332	327.00	0.10360	98.50	1.50	0.252
366	346.71	0.08323	94.73	5.27	0.389

HRT: hydraulic retention time; \bar{t}_c : mean retention time; σ_θ^2 : normalized variance; e: effective volume; V_d : dead volume; SCI: short-circuiting index.

Short-circuiting is an important factor contributing to the low hydraulic efficiency [21,22]. The short-circuiting decreases as the short-circuiting index tends to 1, it rises when the index tends to 0, and its values below 0.3 shows a considerable short-circuiting [3]. Based on this number, it could be stated that a considerable short-circuiting only occurs at the 332-min retention time (Table 1). Similar to the dead volume, there is not a precise relationship between the short-circuiting index and the reactor's retention time, but it seems that the SCI generally decreases as the reactor's retention time grows.

3.2. Investigation of TIS and AD models

The number of equivalent tanks in series at different retention times is presented in Table 2. Considering these values, the distribution curve for tanks in the series model (dot lines in Fig. 2) can be created for each retention time. According to Fig. 2, it could be stated that the TIS model is generally suitable for assessing the behavior of the ABR, especially in higher retention times. Sarathai et al. [3] also considered TIS model as an appropriate model for ABR.

With an increase in the reactor's retention time, conformity of this model to the experimental results increases. Hence, at 284, 332, and 366 min retention times, these two curves almost coincide. However, as shown in Fig. 2b, this model seems to be unsuitable for asymmetric curves.

Based on Table 2, the number of tanks in series does not change considerably with a change in the retention time and thus it is independent of the retention time. Then, the flow regime of ABR is not dependent on HRT. This result is contrary to the opinion of Renuka et al. [18]. By averaging the number of tanks in series, this value becomes 10.89. Considering the higher compliance with the last three retention times, the number of tanks is 10.58. This value is 1.32-fold larger than the number of the reactor's compartments, and thus this conclusion complies with the findings reported by Sarathai et al. [3], who calculated the number of tanks in series to be 4 with a reactor containing 3 compartments. In some studies, the number of tanks in series is assumed to be approximately equal to the number of ABR compartments [17,23]. As a result, the number of tanks in series and subsequently

Table 2
Number of equivalent tanks in TIS model and dimensionless numbers of AD model for various HRTs

HRT (min)	N	d	Pe
93	12.89	0.040	24.7
110	10.13	0.052	19.2
180.2	11.27	0.047	21.5
248	10.21	0.052	19.4
284	10.08	0.052	19.1
332	9.65	0.055	18.2
366	12.01	0.044	22.9

N : the number of tanks in series; d : dispersion number; Pe : Péclet number.

the flow regime type of reactor depends on the number of compartments.

Table 2 shows the Péclet and dispersion numbers for different retention times. Accordingly, they all have high dispersion contents ($d > 0.01$) and the dispersion equation for the high-dispersion state with closed boundaries needs to be solved. Also, the Péclet and dispersion numbers are not considerably different and are almost unchanged at different retention times.

Fig. 2 (dashed lines) compares the axial dispersion model with experimental distribution curves. According to this figure, the axial dispersion model is relatively suitable for the anaerobic baffled reactor. In particular, compared to the TIS model, this model shows better conformity with lower retention times. However, similar to the TIS model, this model is not suitable for the assessment of asymmetrical distribution curves either (Fig. 2b). In this regard, Levenspiel [12] holds the same belief.

Considering the openness or closeness of reactor boundaries precisely and solving the dispersion equation based on suitable boundary conditions are highly important, because misleading solutions will be obtained by solving the equation based on improper boundary conditions. To explain this issue, the results of this research were compared to the study by Sarathai et al. [3]. The aforementioned researchers express that the AD model does not suite anaerobic baffled reactors. They also asserted that the output of the AD model is more symmetrical than the experimental curve and underestimates dispersion content as compared to experimental results. The main weakness of this model is reported to be the late emergence of the curve's peak as compared to the experimental curve. As a result, the overestimation of the mean retention time of AD model may occur [3].

As opposed to findings by Sarathai et al. [3], results of the present study not only introduce the AD model as an almost suitable model but also suggest that the model-produced curve's peak time nearly equals that of experimental curve's peak time with a small deviation. The difference between the model-produced and experimental curves' peak times in the present study is very slight and almost negligible as compared to the research by Sarathai et al. [3].

The reason for the difference between results of these two studies is that Sarathai et al. [3] assumed open

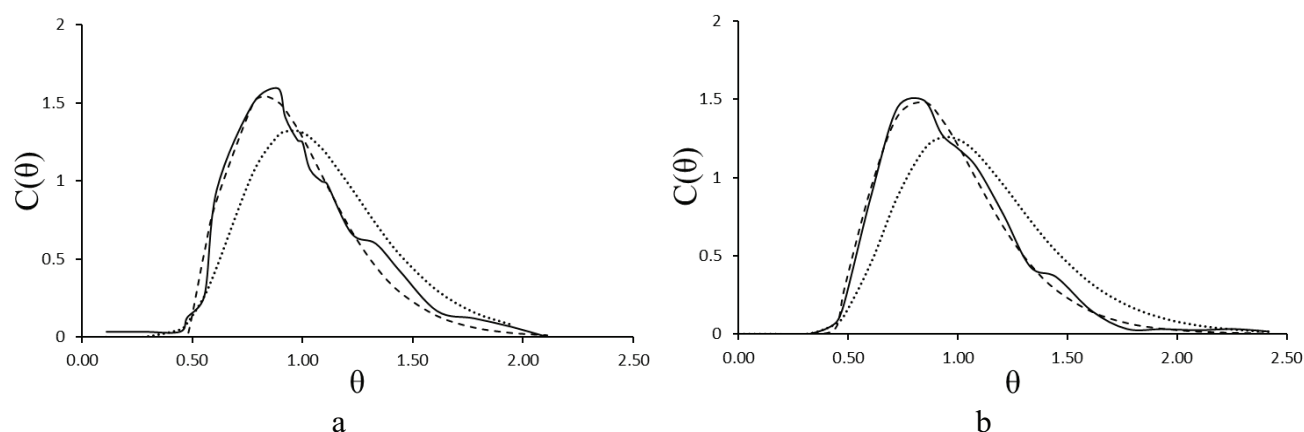


Fig. 3. Misleading conclusions brought about by open assumption of reactor's boundary conditions (a: 180 min, b: 248 min). The Solid lines refer to Experimental RTD curves, the dashed lines refer to closed boundaries assumption (correct) and the dot lines refer to open boundaries assumption (incorrect).

boundaries and solved the dispersion model for open boundary conditions, while the ABR is a reactor with closed boundaries.

In Fig. 3, the experimental curve is plotted along with the resulting curve from the equation solved for closed boundaries (as assumed in this research) and the resulting curve from the equation solved for open boundaries (as assumed by Sarathai et al. [3]) at 180 and 248-min retention times. According to Fig. 3, the curve obtained for the reactor modeled with closed boundaries almost conforms to the experimental curve. While the curve obtained with the open boundaries does not comply with experimental results. Moreover, the curve peak time for the open boundaries is bigger than the experimental peak time, which complies with findings of Sarathai et al. [3]. However, this result is misleading and is obtained because the reactor's boundaries, which are actually closed, are assumed to be open. If the boundary assumption is made correctly, the model's curve and the experimental curve will conform.

3.3. Determining the flow regime of reactor

The flow regime type of the reactor is determined using the number of equivalent tanks in series or the dispersion number. If the dispersion number moves toward infinity or if the number of tanks is close to 1, the reactor becomes more similar to a completely mixed reactor; however, if the dispersion number moves toward zero and the number of tanks moves toward infinity, the reactor becomes more like a plug flow reactor. In addition, in case the TIS model is used, if the number of tanks is smaller than or equal to 3, the dispersion is assumed to be high. In the AD model, the Péclet number of 5 is considered as the threshold value, below which a considerable dispersion is seen [24]. In view of these criteria and values presented in Table 3, ABR demonstrates low dispersion using both models and tends to be a plug flow reactor. Moreover, the reactor's flow regime is not related to its hydraulic retention time. Fig. 1b depicts the tracer experiment in this research. Dispersion of the tracer in the upward and downward sections is evident in this figure. Considering the uniform distribution of the

Table 3
Plug flow index, plug flow and completely mixed volumes and hydraulic efficiency for various HRTs

HRT (min)	PI (TIS)	PI (AD)	V_p (%)	V_m (%)	λ (%)
93	0.92	0.92	85.63	4.30	82.95
110	0.90	0.91	77.75	11.10	80
180.2	0.91	0.91	89.94	8.78	90
248	0.90	0.91	87.52	9.23	87.27
284	0.90	0.91	92.46	10.36	92.62
332	0.90	0.90	88.30	10.19	88.29
366	0.92	0.92	88.67	6.05	86.84

PI: plug flow index; V_p : plug flow volume; V_m : completely mixed volume; λ : hydraulic efficiency.

tracer in the downward section, it could be stated that this section significantly contributes to the plug nature of the flow. A recent study also confirmed this conclusion [5].

The above-mentioned categorization of flow types is incapable of an exact comparison between two plug flow (or two completely mixed) reactors. In this paper, to provide a better understanding and comparability of reactor flow types, the "plug flow index" was proposed in the form of Eq. (21) and Eq. (22) for the TIS and AD models, respectively.

$$PI = \frac{N-1}{N} \quad (21)$$

$$PI = \frac{1}{1+2d} = \frac{Pe}{Pe+2} \quad (22)$$

In the above equations, PI is the plug flow index, which varies between zero and one. Moreover, N , d , and Pe are the number of equivalent tanks in series, dispersion number, and Péclet number, respectively.

Based on the mentioned index, reactors are classified into the following three categories:

A) Plug flow reactors ($PI > 0.75$)

Reactors of this group perform in a very similar manner to ideal plug flow reactors, and the existing flow in these reactors can be considered as plug type. If $N > 4$ or $Pe > 6$ or $d < 0.167$, the reactor is considered to be a plug flow reactor.

B) Intermediate reactors ($0.5 < PI \leq 0.75$)

The performance of these reactors is between ideal completely mixed and ideal plug flow reactors. In other words, the flow is not exactly similar to or different from each of them. If $N = 3$ and 4 or $2 < Pe \leq 6$ or $0.167 \leq d < 0.5$, the reactor is an intermediate reactor.

C) Completely mixed reactors ($PI \leq 0.5$)

Characteristics of flows in these reactors are very similar to those of flows in the ideal completely mixed reactors with a high dispersion. In this regard, if $N = 1$ and 2 , or $Pe \leq 2$ or $d \geq 0.5$, the reactor is a completely mixed reactor.

The plug flow indices for the TIS and AD models at different retention times are shown in Table 3. Based on this table, the anaerobic baffled reactor used in this study is a plug flow reactor with a high PI index (higher than 0.9). Also, the volume in which the reactor acts as a plug flow

reactor is much more than the volume supporting the completely mixed characteristics.

According to Eq. (20), as the number of reactor's equivalent tanks in series grows, a better efficiency is yielded. In other words, the reactor's efficiency increases as the reactor becomes more similar to an ideal plug flow reactor; which is among the advantages of plug flow reactors. A hydraulic efficiency value larger than 0.75 is considered to be a high efficiency [24]. Therefore, according to Table 3, the reactor yields high efficiency in all retention times.

3.4. Analysis of actual fluid conditions

The effect of temperature, dissolved solids, and suspended solids was investigated to analyze the actual flow conditions. The HRT was 180 min (as a typical HRT) in all experiments and the results are presented as follow.

3.4.1. Effect of temperature

Fig. 4a shows the RTD curves at 10 and 30°C temperatures along with the experimental curve obtained at room temperature (22°C). According to the figure, with an increase in temperature, the curve distribution expands more and the curve becomes less similar to that of a plug flow. According to Table 4, the number of equivalent tanks

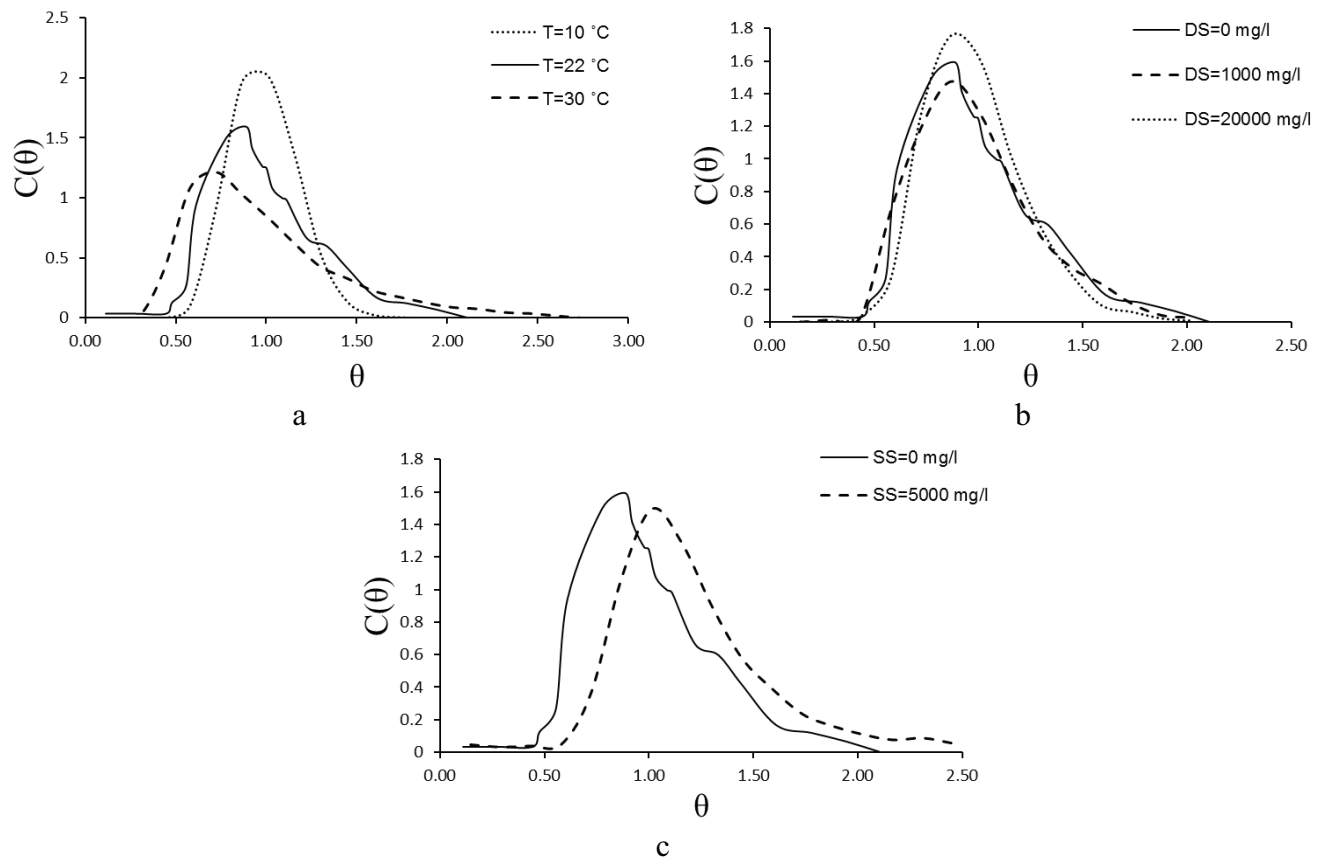


Fig. 4. The effects of circumstances variation on RTD curves. a: The effect of temperature (T is temperature), b: The effect of dissolved solids (DS is dissolved solids), c: The effect of suspended solids (SS is suspended solids).

Table 4
Hydrodynamic characteristics of ABR in various temperatures and HRT = 180 min

Temp (°C)	\bar{t}_c (min)	σ_g^2	e (%)	V_d (%)	SCI	N	λ (%)	Pe	d	PI (TIS)	PI (AD)
10	177.8	0.03543	98.78	1.22	0.585	28.22	95	55.43	0.018	0.96	0.96
22	177.9	0.08877	98.72	1.17	0.45	11.27	90	21.48	0.047	0.91	0.91
30	178	0.1867	98.89	1.11	0.382	5.36	80	9.6	0.104	0.81	0.83

Table 5
Hydrodynamic characteristics of ABR in various dissolved solids and HRT = 180 min

DS (mg/)	\bar{t}_c (min)	σ_g^2	e (%)	V_d (%)	SCI	N	λ (%)	Pe	d	PI (TIS)	PI (AD)
–	177.9	0.08877	98.72	1.28	0.45	11.27	90	21.5	0.047	0.91	0.91
1000	177.74	0.09252	98.75	1.25	0.439	10.81	90	20.57	0.049	0.91	0.91
20000	177.14	0.06043	98.41	1.59	0.44	16.55	92	32.06	0.031	0.94	0.94

Table 6
Hydrodynamic characteristics of ABR in various suspended solids and HRT = 180 min

TSS (mg/)	\bar{t}_c (min)	e (%)	V_d (%)	SCI	N	λ (%)	Pe	d	PI (TIS)	PI (AD)
–	177.9	98.72	1.28	0.483	11.27	90	21.5	0.047	0.91	0.91
5000	215.45	–	–	0.511	11.1	–	21.15	0.047	0.92	0.91

in series and the Pécet number decrease considerably and the dispersion number increases with rising temperature. This result shows the reactor's tendency to become a completely mixed reactor. The number of equivalent tanks in series reduces more than 5 times with a 20°C increase in temperature. The plug flow index (PI) also declines considerably with a rise in temperature, which shows the reactor's tendency to become a completely mixed reactor. As temperature changes from 22 to 30°C, the number of equivalent tanks in series decreases and hydraulic efficiency declines by 10%. However, as temperature drops from 22 to 10°C, hydraulic efficiency grows by 5%. It seems that the reactor's flow type tends to be similar to an ideal completely mixed reactor and dispersion increases with the increase in temperature. This behavior could be explained by the increasing movement of fluid molecules. This result is contrary to that reported by Langenhoff and Stuckey [23], who believed the reactor tends to be a plug flow reactor with an increase in temperature. The time of tracer's first appearance at the reactor's outlet as well as the curve peak time decreased with increasing temperature (Fig. 4a), but the mean retention time remained unchanged with temperature fluctuations (Table 4). The decrease in the first tracer outgoing time with increasing temperature reflects a decrease in the SCI and an increase in the probability of short-circuiting. Since the mean retention time remains constant, the reactor's effective and dead spaces also remain unchanged. Hence, it could be concluded that reactor's dead volume is not related to fluid temperature. This conclusion is similar to the finding by Langenhoff and Stuckey [23]. As a practical result, the decrease in temperature negatively affects the reactor's performance due to its adverse effects on microorganisms' performance. In comparison, the hydrodynamic indices are improved as

temperature drops, and this outcome may somewhat compensate for the negative effects.

3.4.2. Effect of dissolved solids

To simulate the effect of dissolved solids on the flow, solutions with 1000 and 20000 mg/L concentrations were tested. The related RTD curves are depicted in Fig. 4b along with the curve for water without solutes. Obviously, only considerable changes in solutes content influence the reactor's flow regime. Concerning changes of mean retention time, dead and effective spaces, and the SCI (Table 5), it could be stated that the values showed no significant changes in any of the above states. Hence, a considerable increase in dissolved solids drives the reactor toward ideal plug flow reactors, while other reactor hydrodynamic indices are not affected by solutes.

3.4.3. Effect of suspended solids

Fig. 4c shows a comparison between RTD curve of suspended solids with a concentration of 5000 mg/L and the curve for water without suspended solids (potable water). It has to be noted that an experiment with a suspended solids concentration of 250 mg/L was also carried out, but it was omitted from the diagram due to lack of major changes in the resulted curve. The curve for the water sample with suspended solids does not significantly differ from the potable water curve except that it is transferred to the positive side of the time axis. Due to the curve distribution and a constant variance, the flow regime remained invariant (Table 6). Moreover, after adding the suspended solids, a delay was observed

in tracer outgoing from the reactor, suggesting a decrease in the short-circuiting probability.

4. Conclusions

- The largest dead space obtained in this research was about 11%. The hydraulic dead space decreases with the increase of retention time.
- In most of the test times, no considerable short-circuiting was observed. However, this phenomenon should be noticed especially at higher retention times.
- The reactor applied in this work is highly similar to plug flow reactors. The reactor's flow regime depends on the number of compartments but not depends on the hydraulic retention time. In addition, the reactor could be modeled using the TIS and AD models with a satisfactory approximation.
- The hydraulic efficiency of this reactor was high for all test retention times. This high efficiency is the result of the small hydraulic dead space and a large number of equivalent tanks in series.
- Temperature changes do not influence the reactor's effective and dead volumes. However, the probability of occurrence of short-circuiting grows and reactor's hydraulic efficiency drops with a rise in temperature. In addition, the flow regime becomes similar to the completely mixed flow regime with an increase in temperature.
- Presence of considerable amounts of dissolved solids in the reactor's passing flow can lead the reactor to plug flow types. Also, the presence of solutes does not affect the reactor's dead space and the short-circuiting is not related to the solutes content. Finally, although the presence of suspended solids does not influence the flow regime, it reduces the probability of occurrence of short-circuiting.

Acknowledgments

The authors wish to acknowledge Dr. G. Badalians Golikandi (SBU) as well as Dr. Sh. Jamshidi (Water Research Institute) for academic and technical support.

Symbols

θ	— Normalized time
$\bar{\theta}$	— Normalized mean retention time
θ_{peak}	— Peak time of the RTD curve
σ_{θ}^2	— Normalized variance
λ	— Hydraulic efficiency
C_{θ}	— Normalized concentration at time θ
$C_{(t)}$	— Concentration at time t ,
C	— Concentration
C_0	— Nominalized concentration
C_1	— Concentration in upstream the input boundary
D	— Axial dispersion coefficient
e	— Reactor's effective volume
HRT	— Hydraulic retention time (theoric)

L	— Length
N	— Number of tanks in series
Pe	— Péclet number
PI	— Plug flow index
SCI	— Short-circuiting index
t	— Time
t_i	— Time at which the first output tracer is observed
t_c	— Mean retention time
u	— Flow velocity
V	— Total reactor volume
V_d	— Reactor's dead volume
V_m	— Completely mixed volume
V_p	— Plug flow volume
X	— Distance from the inlet of the reactor
Z	— Normalized length

References

- [1] G. Zhu, R. Zou, A.K. Jha, X. Huang, L. Liu, C. Liu, Recent developments and future perspectives of anaerobic baffled bioreactor for wastewater treatment and energy recovery, *Crit. Rev. Env. Sci. Tec.*, 45 (2015) 1243–1276.
- [2] A. Bachmann, V.L. Beard, P.L. McCarty, Performance characteristics of the anaerobic baffled reactor, *Water. Res.*, 19 (1985) 99–106.
- [3] Y. Sarathai, T. Koottatep, A. Morel, Hydraulic characteristics of an anaerobic baffled reactor as on site wastewater treatment system, *J. Environ. Sci. China*, 22 (2010) 1319–1326.
- [4] S. Li, J. Nan, H. Li, M. Yao, Comparative analyses of hydraulic characteristics between the different structures of two anaerobic baffled reactors (ABRs), *Ecol. Eng.*, 82 (2015) 138–144.
- [5] S. Li, J. Nan, F. Gao, Hydraulic characteristics and performance modeling of a modified anaerobic baffled reactor (MABR), *Chem. Eng. J.*, 284 (2016) 85–92.
- [6] A. Arvin, M. Peyravi, M. Jahanshahi, H. Salmani, Hydrodynamic evaluation of an anaerobic baffled reactor for landfill leachate treatment, *Desal. Water Treat.*, 57 (2016) 19596–19608.
- [7] M. Xu, L. Ding, K. Xu, J. Geng, H. Ren, Flow patterns and optimization of compartments for the anaerobic baffled reactor, *Desal. Water Treat.*, 57 (2016) 345–352.
- [8] W.P. Barber, D.C. Stuckey, The use of the anaerobic baffled reactor (ABR) for wastewater treatment: a review, *Water Res.*, 33 (1999) 1559–1578.
- [9] R. Liu, Q. Tian, J. Chen, The developments of anaerobic baffled reactor for wastewater treatment: A review, *Afr. J. Biotechnol.*, 9 (2010) 1535–1542.
- [10] P. Dama, J. Bell, C.J. Brouckaert, C.A. Buckley, D.C. Stuckey, Computational fluid dynamics: application to the design of the anaerobic baffled reactor, *Proc. WISA Biennial Conference*, 2000, Sun City, South Africa.
- [11] Metcalf & Eddy Inc., G. Tchobanoglous, H.D. Stensel, R. Tsuchihashi, F. Burton, *Wastewater Engineering: Treatment and Resource Recovery*, McGraw-Hill, New York, 2013.
- [12] O. Levenspiel, *Chemical Reaction Engineering*, John Wiley & Sons. Inc, New York, 1999.
- [13] X. Chen, P. Zheng, Y. Guo, Q. Mahmood, C. Tang, S. Ding, Flow patterns of super-high-rate anaerobic bioreactor, *Bioresour. Technol.*, 101 (2010) 7731–7735.
- [14] Y.K. Ahn, A diffusion model of an isothermal tubular flow reactor, Master's Thesis. Kansas State University, USA. 1962.
- [15] T.T. Ren, Y. Mu, H.Q. Yu, H. Harada, Y.Y. Li, Dispersion analysis of an acidogenic UASB reactor, *Chem. Eng. J.*, 142 (2008) 182–189.
- [16] J. Persson, N.L.G. Somes, T.H.F. Wong, Hydraulic efficiency of constructed wetlands and ponds, *Water Sci. Technol.*, 40(1999) 291–300.
- [17] A. Grobicki, D.C. Stuckey, Hydrodynamic characteristics of the anaerobic baffled reactor, *Water. Res.*, 26 (1992) 371–378.

- [18] R. Renuka, S. Mariraj Mohan, S. Amal Raj, Hydrodynamic behaviour and its effects on the treatment performance of panelled anaerobic baffle-cum filter reactor, *Int. J. Environ. Sci. Technol.*, 13 (2016) 307–318.
- [19] X. Liu, N. Ren, C. Wan, Hydrodynamic characteristics of a four-compartment periodic anaerobic baffled reactor, *J. Environ. Sci. China*, 19 (2007) 1159–1165.
- [20] H.W. Young, J.C. Young, Hydraulic characteristics of upflow anaerobic filters, *J. Environ. Eng.*, 114 (1988) 621–928.
- [21] F.E. Dierberg, J.J. Juston, T.A. DeBusk, K. Pietro, B. Gu, Relationship between hydraulic efficiency and phosphorus removal in a submerged aquatic vegetation-dominated treatment wetland, *Ecol. Eng.*, 25 (2005) 9–23.
- [22] S. Singh, R. Haberl, O. Moog, R.R. Shrestha, P. Shrestha, R. Shrestha, Performance of an anaerobic baffled reactor and hybrid constructed wetland treating high-strength wastewater in Nepal—A model for DEWATS, *Ecol. Eng.*, 35 (2009) 654–660.
- [23] A.A.M. Langenhoff, D.C. Stuckey, Treatment of dilute wastewater using an anaerobic baffled reactor: effect of low temperature, *Water Res.*, 34 (2000) 3867–3875.
- [24] J. Ji, K. Zheng, Y. Xing, P. Zheng, Hydraulic characteristics and their effects on working performance of compartmentalized anaerobic reactor, *Bioresource Technol.*, 116 (2012) 47–52.